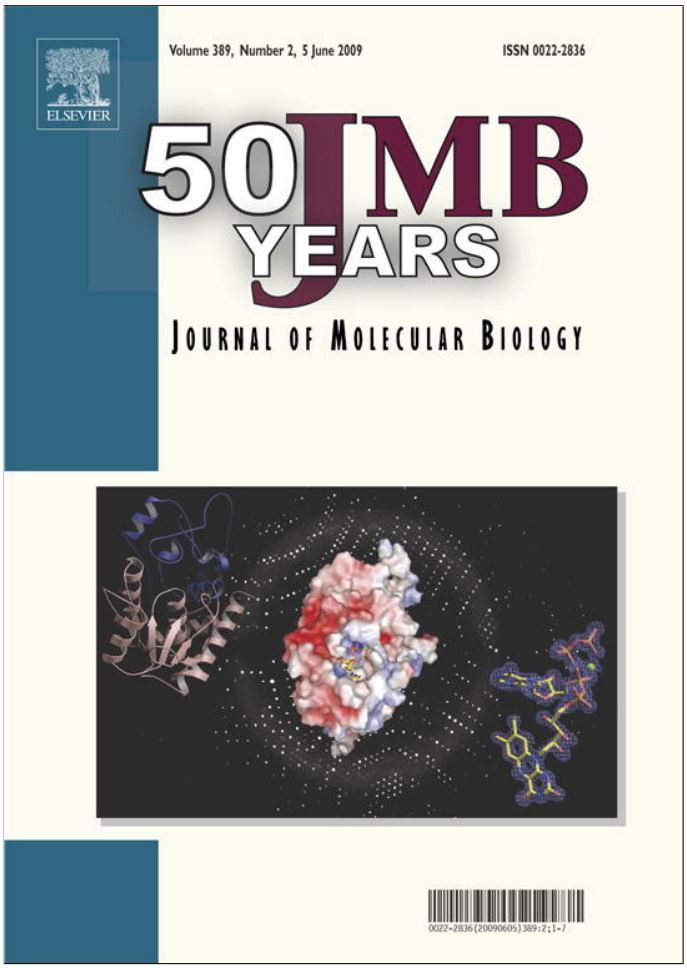

doi:10.1016/j.jmb.2009.04.013 J. Mol. Biol. (2009) 389, 306–314

JMB

Available online at www.sciencedirect.com

ScienceDirect

ELSEVIER

Substrate Shuttling between Active Sites of Uroporphyrinogen Decarboxylase Is Not Required to Generate Coproporphyrinogen

John D. Phillips[1]*, Christy A. Warby[1], Frank G. Whitby[2], James P. Kushner[1] and Christopher P. Hill[2]

[1]*Department of Medicine, University of Utah School of Medicine, 5C330 SOM, 30 North 1900 East, Salt Lake City, UT 84132, USA*

[2]*Department of Biochemistry, University of Utah School of Medicine, Salt Lake City, UT 84132, USA*

Received 27 January 2009; received in revised form 31 March 2009; accepted 1 April 2009
Available online 10 April 2009

Uroporphyrinogen decarboxylase (URO-D; EC 4.1.1.37), the fifth enzyme of the heme biosynthetic pathway, is required for the production of heme, vitamin B12, siroheme, and chlorophyll precursors. URO-D catalyzes the sequential decarboxylation of four acetate side chains in the pyrrole groups of uroporphyrinogen to produce coproporphyrinogen. URO-D is a stable homodimer, with the active-site clefts of the two subunits adjacent to each other. It has been hypothesized that the two catalytic centers interact functionally, perhaps by shuttling of reaction intermediates between subunits. We tested this hypothesis by construction of a single-chain protein (single-chain URO-D) in which the two subunits were connected by a flexible linker. The crystal structure of this protein was shown to be superimposable with wild-type activity and to have comparable catalytic activity. Mutations that impaired one or the other of the two active sites of single-chain URO-D resulted in approximately half of wild-type activity. The distributions of reaction intermediates were the same for mutant and wild-type sequences and were unaltered in a competition experiment using I and III isomer substrates. These observations indicate that communication between active sites is not required for enzyme function and suggest that the dimeric structure of URO-D is required to achieve conformational stability and to create a large active-site cleft.

Published by Elsevier Ltd.

Keywords: uroporphyrinogen decarboxylase; porphyria; heme biosynthesis; porphyrinogen; enzyme mechanism

Edited by M. Guss

Introduction

Biosynthesis of heme requires a complex multienzyme process that is distributed between mitochondria and cytosol. The fifth enzyme of this pathway, cytosolic uroporphyrinogen decarboxylase (URO-D; EC 4.1.1.37), catalyzes the decarboxylation of four acetate side chains of uroporphyrinogen (uro'gen) to generate coproporphyrinogen (copro'gen). The biologically relevant URO-D substrate is the uro'gen III isomer, although uro'gen I, which is produced in the absence of adequate activity of the preceding uro'gen III synthase enzyme, is also a substrate. The copro'gen I product, however, cannot be converted into protoporphyrinogen and, ultimately, heme. Mechanistic studies have shown that there is an ordered decarboxylation of uro'gen III beginning at the asymmetric D-ring and proceeding sequentially to rings A, B, and C (Fig. 1).[1] URO-D is encoded by a single gene[2] and is essential for the synthesis of heme and chlorophyll.[3] Subnormal activity of URO-D in hepatocytes is the cause of the most common form of porphyria in humans, porphyria cutanea tarda.[4]

URO-D forms a stable homodimer[5] in which each subunit adopts a $(\beta/\alpha)_8$-barrel structure.[6] Each subunit contains a deep active-site cleft, and the two active sites in the dimer are juxtaposed such that the two clefts are largely contiguous. Crystal structures of URO-D, in complex with the copro'gen reaction

*Corresponding author. E-mail address: john.phillips@hsc.utah.edu.

Abbreviations used: URO-D, uroporphyrinogen decarboxylase; uro'gen, uroporphyrinogen; copro'gen, coproporphyrinogen; HIS, 10× histidine tag; CBD, cellulose-binding domain; scURO-D, single-chain URO-D; PDB, Protein Data Bank.

0022-2836/$ - see front matter. Published by Elsevier Ltd.

product, revealed that the product tetrapyrrole macrocycle adopts a domed conformation that lies against a collar of conserved hydrophobic residues and allows formation of hydrogen-bonding interactions between a carboxylate oxygen atom of the invariant Asp86 side chain and the four pyrrole NH groups.[7] These structural data and associated biochemical analyses of mutant URO-D proteins indicate a critical role for Asp86 in substrate binding and promotion of catalysis by stabilizing a positive charge on a reaction intermediate.[7] This model may explain why, unlike many decarboxylases, URO-D does not utilize a cofactor. Furthermore, the central coordination geometry of Asp86 allows initial substrates and various partially decarboxylated intermediates to bind with similar activating interactions. Although the precise site of decarboxylation remains uncertain, this binding geometry strongly suggests that all four of the substrate acetate groups are decarboxylated by the same mechanism.

Although the active site in each URO-D subunit appears capable of performing all of the decarboxylation reactions that are required to form the ultimate product, apposition of active sites within the dimer suggested the possibility that partially decarboxylated reaction intermediates might shuttle between subunits. This idea was especially attractive for the second decarboxylation reaction of the III isomer substrate because the asymmetric structure of 7-carboxy porphyrinogen III would not permit this structure to bind with the reactive pyrrole acetate, propionate, and NH groups at the active site by a simple rotation within a single active site. Decarboxylation of 7-carboxy porphyrinogen III could result from dissociation and rebinding with its opposite face against the enzyme, or it could dissociate and be repositioned in the adjacent active site without the need to flip and reorient the opposite face of the substrate in the active site. It has also been suggested that once the substrate is bound, all four of the decarboxylation events are performed using the same catalytic residues without the need for the intermediate to leave the substrate-binding pocket. Once all four decarboxylation events have been performed, the product would be able to exit the binding pocket.[8]

To determine whether enzyme activity requires that partially decarboxylated reaction intermediates shuttle between subunit active sites without completely dissociating from URO-D, we expressed and purified a single-chain form of a URO-D dimer. In this protein, the two monomeric domains are joined by a linker from the C-terminus of one URO-D to the N-terminus of the second URO-D. This single-chain dimer behaved as an authentic wild-type dimer by gel-filtration chromatography, analytical ultracentrifugation, crystal structure, and enzyme activity. Variants of the linked dimer in which either of the active sites was inactivated by site-directed mutagenesis maintained approximately half of the wild-type catalytic activity. Moreover, wild-type and mutant proteins displayed very similar distributions of reaction intermediates. These data indicate that all four decarboxylations can be catalyzed at a single active site and that shuttling of intermediates between active sites of the URO-D dimer is not required.

Results and Discussion

scURO-D: A single-chain URO-D dimer

To establish the catalytic requirement for a dimeric structure of URO-D, we constructed a monomeric single subunit variant by mutating residues that stabilize the dimer interface. Six different mutant URO-D proteins were constructed; however, in all cases, they were insoluble (data not shown), consistent with the model that dimer formation is important for URO-D folding and/or conformational stability. We next took the approach of expressing URO-D proteins with two different tags—a 10× histidine tag (HIS) or a cellulose-binding domain (CBD)—within the same host strain of *Escherichia coli*. Both tagged versions of URO-D were expressed in approximately equal

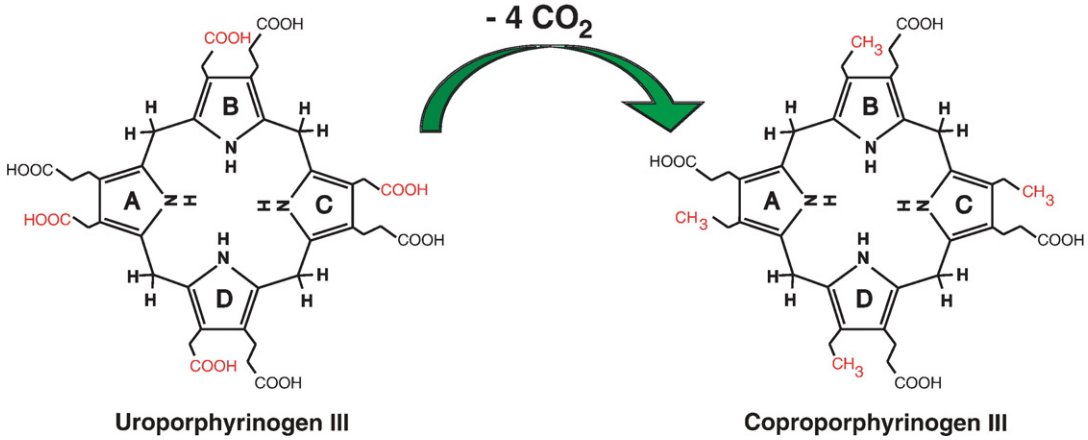

Fig. 1. Reaction catalyzed by URO-D. The four acetate groups of uro'gen are decarboxylated to form methyl groups and four molecules of CO_2. Decarboxylation begins with the D-ring and proceeds clockwise to the A-, B-, and C-rings.

Table 1. Activity of scURO-D proteins

Construct	*n*	Activity	SE	% URO-D	% scURO-D
Uro'gen I activity					
URO-D	6	4364	188	100.0	133.9
Y164G URO-D	3	353	49	8.1	10.8
F217Y URO-D	4	114	18	2.6	3.5
scURO-D	6	3260	143	74.7	100.0
scURO-D(FY)	6	1802	40	41.3	55.3
scURO-D(YF)	6	2014	128	46.2	61.8
scURO-D(YY)	4	107	5	2.5	3.3
scURO-D(GY)	2	578		13.2	17.7
Uro'gen III activity					
URO-D	6	8028	913	100.0	117.7
scURO-D	6	6821	662	85.0	100.0
scURO-D(FY)	6	4087	320	50.9	59.9
scURO-D(YF)	6	4229	330	52.7	62.0
scURO-D(YY)	4	1163	62	14.5	17.1

Uro'gen III, uroporphyrinogen III at 30 nM; *n*, number of independent assays performed in duplicate; activity, average activity as nanomoles of product per hour per milligram of protein.

amounts, and the recovery of the properly folded proteins was equal to that observed for the single-vector system. However, the percentage of dimers containing both tags (HIS and CBD) was very small (data not shown). These data suggest that formation of the dimer is cotranslational (from the same polysome), as has been described for p53,[9] and that little subunit exchange takes place. These properties and interactions lead to the formation of a stable homodimer with a half-life of more than 80 h.[10] We then expressed and purified each of the differentially tagged proteins individually. Equal molar ratios of the two proteins were mixed and allowed to equilibrate at various temperatures and concentrations. Results from this experiment were similar to those of the dual-expression system in that very little of the repurified protein contained both purification tags.

We therefore took an alternative approach in which two separate active sites are housed within a single dimeric URO-D molecule. Use of this single-polypeptide approach eliminated any confounding variables due to subunit exchange between wild-type and mutant monomers. This was performed by constructing single-chain variants [single-chain URO-D (scURO-D)] in which two human URO-D monomers were connected by a flexible linker sequence. Linkers were designed based on inspection of the wild-type URO-D crystal structure,[6] which showed that the N-termini and C-termini of the two subunits in a dimer are separated by approximately 75 Å when measured by the shortest path along the surface of the molecule. Linkers containing the 10× His affinity tag and are rich in Gly and Ser residues comprising 29, 33, 35, and 37 residues were designed. These constructs were expressed, and proteins were purified and tested for enzymatic activity. Maximal activity was observed for the 35-residue linker protein. This optimally active construct, referred to simply as scURO-D, and its point mutant variants were used in all of the subsequent biochemical and structural studies. scURO-D displayed 75% and 85% of wild-type protein activity when assayed against uro'gen I and uro'gen III isomer substrates, respectively (Table 1). This statistically significant ($p = 0.01$) loss (25%) of activity presumably results from a subtle conformational restriction, but does not result from a fundamental change in mechanism, as indicated by the conserved profile of reaction intermediates and the effect of active-site mutants (see the text below).

Purified scURO-D protein with ~80% of wild-type activity migrates at almost the same position as wild-type URO-D on a sizing column. scURO-D preparations are contaminated (10–20%) by protein that has been clipped in the linker region (Fig. 2), as indicated by N-terminal sequencing of the two species present (data not

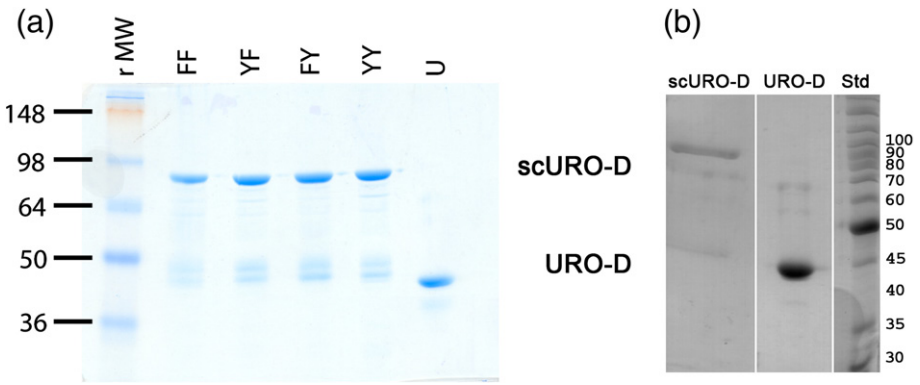

Fig. 2. Purified proteins. (a) A 1-μg sample of each of the purified proteins visualized on Coomassie-stained SDS-PAGE: scURO-D (YY), scURO-D(YF) (YF), scURO-D(FY) (FY), scURO-D(FF) (FF), and URO-D (U). The scURO-D proteins have an apparent molecular mass of 84 kDa, while native URO-D runs at 42 kDa. The densitometry of the bands present in the scURO-D sample indicated that approximately 10–20% of the URO-D protein is present at the molecular mass corresponding to that of monomeric URO-D. (b) Crystals of scURO-D were removed from the crystallization well, washed, and dissolved in 50 mM Tris (pH 7.5). Proteins were separated by SDS-PAGE. The densitometry of the bands present in the scURO-D sample indicated that approximately 22% of the protein is present at a molecular mass corresponding to that of monomeric URO-D.

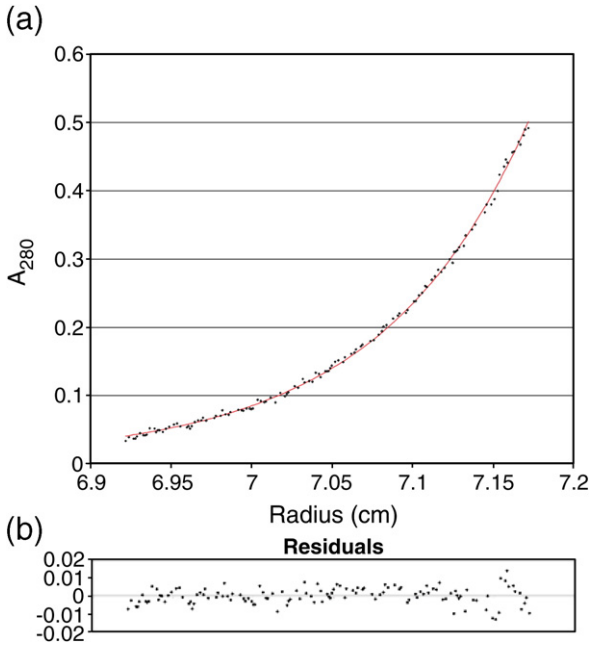

Fig. 3. Analytical ultracentrifugation of scURO-D. Samples of scURO-D at 0.25 and 0.08 mg/mL were placed in two chambers of the centrifuge cell of a Beckman XL-A and spun at 12,000 rpm at 20 °C to equilibrium. All data were fitted globally to a monomer, resulting in a predicted molecular mass of 85,972 Da, consistent with the expected mass of the scURO-D (85,497 Da). (a) Points represent 268 averaged data values from five scans (A_{280}). The continuous line is the best globally fitted model. (b) Residuals for the scan shown in (a).

shown). In order to rigorously verify the oligomeric state of scURO-D, the purified protein was analyzed by equilibrium analytical ultracentrifugation. scURO-D protein sedimented as a single homogeneous species of 86 kDa (Fig. 3), consistent with equivalent data obtained for the wild-type protein and indicating that scURO-D adopts the designed structure.

Further evidence indicating that the scURO-D structure is not substantially distorted from the wild type by the linker was provided by crystal structure determination to a resolution of 2.1 Å and an R_{free} value of 0.245 (Table 2). Crystals were isomorphous with wild-type URO-D crystals (Supplementary Fig. 1). This was not expected, as the space group $P3_121$ contains just one URO-D subunit in the asymmetric unit, with the dimer built by application of a crystallographic 2-fold axis, whereas the two domains of scURO-D differ by the presence of linker residues at their N- or C-termini. The structure was therefore built as if the two scURO-D domains were stochastically distributed on either side of the crystallographic 2-fold axis (i.e., with full occupancy for groups that are present in both domains and with half occupancy for groups that are unique to the linker region, almost all of which are disordered and lack density) (Supplementary Fig. 2). This solution was supported by refinement and inspection of Fourier maps using the highly redundant data processed in the lower symmetry space group $P3$. The predominant presence of uncleaved scURO-D in the crystal was confirmed by visualization of washed crystals on SDS-PAGE (Fig. 2). The $P3_121$ space group is accommodated because, although the N-terminal and C-terminal URO-D modules are distinguished by unique flanking sequences, they are otherwise identical, and the crystal lattice contacts are mediated by segments common to both domains. The refined scURO-D and native URO-D models superimpose

Table 2. Data collection and refinement statistics for scURO-D proteins

Data set	scURO-D	scURO-D(GY)	scURO-D(FY)	scURO-D(YF)
Wavelength (Å)	1.5418	1.5418	1.5418	1.5418
Resolution (Å)[a]	30.0–2.10 (2.16–2.10)	30.0–2.20 (2.26–2.20)	40.0–2.80 (2.90–2.80)	40.0–2.80 (2.90–2.80)
Number of Reflections reflections measured	129,445	135,250	131,959	83,299
Number of unique reflections	25,394	22,288	10,977	11,174
Completeness (%)	98.0 (86.3)	99.3 (98.6)	98.1 (85.9)	100.0 (100.0)
$\langle I/\sigma I\rangle$	10 (2.3)	8.5 (2.0)	9.5 (1.9)	10.2 (1.9)
Mosaicity (°)	0.91	1.10	0.39	0.85
R_{sym}[b] (%)	0.070 (0.553)	0.110 (0.395)	0.183 (0.455)	0.086 (0.704)
Number of protein residues modeled	11–366	11–366	11–366	11–366
Number of water molecules	145	125	23	24
$\langle B\rangle$ protein (Å^2)	40.0	39.8	48.4	68.6
$\langle B\rangle$ main chain (Å^2)	39.1	39.0	47.3	67.7
$\langle B\rangle$ water (Å^2)	44.6	44.4	66.6	87.5
R_{cryst}[c] (%)	0.193 (0.244)	0.193 (0.245)	0.169 (0.264)	0.193 (0.282)
R_{free} (%)[d]	0.231 (0.321)	0.234 (0.297)	0.223 (0.396)	0.239 (0.338)
RMSD bond lengths (Å)/angles (°)	0.014/1.265	0.012/1.293	0.020/1.922	0.023/2.204

[a] Values in parentheses refer to the highest-resolution shell.
[b] $R_{sym} = \sum |I - \langle I\rangle| / \sum I$, where I is the intensity of an individual measurement, and $\langle I\rangle$ is the corresponding mean value.
[c] Crystallographic R-value (R_{cryst}) $= \sum ||F_o| - |F_c|| / \sum |F_o|$, where $|F_o|$ is the observed structure factor amplitude and $|F_c|$ is the calculated structure factor amplitude.
[d] R_{free} is the same as R_{cryst}, calculated with a randomly selected test set of reflections that were never used in refinement calculations. For each refinement, the following numbers of reflections were chosen for the test set: scURO-D, 1298; scURO-D(GY), 1145; scURO-D(FY), 1067; scURO-D(YF), 1086.

with an RMSD of 0.197 Å over 332 of 357 of the subunit C^{α} atoms.

Design and characterization of inactive mutants

It was expected that if substrate shuttling between active sites were required, mutants that prevented binding of substrate or any of the intermediates would be less informative than constructed mutants that could bind substrates but were catalytically inactive. We previously identified phenylalanine 217 and tyrosine 164 as active-site residues.[7] Enzymatic activity of mutant proteins showed that F217Y URO-D possesses negligible (2.6%) activity when assayed with uro'gen I and that Y164G URO-D retains only 8.1% activity when assayed with uro'gen I (Table 1). The single-chain dimer construct was reengineered to encode the F217Y mutation in the active site of the first module [scURO-D(YF)], in the active site of the second module [scURO-D(FY)], and in the active sites of both modules [scURO-D (YY)]. Another single-chain dimer construct was re-engineered to encode the Y164G mutation in the active site of the first module [scURO-D(YG)]. As discussed below, scURO-D(YG) was especially valuable in confirming the crystallographic assignment of the mutant proteins. In common with other mutant URO-D proteins (data not shown), it was noticed that F217Y URO-D proteins fluoresced upon illumination by UV light, suggesting that porphyrins were bound. A sample of each F217Y protein was denatured by heating, and the eluted porphyrins were analyzed by high-performance liquid chromatography (HPLC). Coproporphyrin was found to be the major porphyrin detected along with minor amounts of partially decarboxylated porphyrins. This ability of the F217Y mutant proteins to bind reaction intermediates and products is consistent with the retention of small but measurable levels of enzyme activity.

In order to rigorously verify that mutation of F217 or Y164 does not inactivate scURO-D by gross disruption of the structure, we determined the crystal structures of scURO-D(GY), scURO-D(YF), and scURO-D(FY). The structures were refined at resolutions of 2.2, 2.8, and 2.8 Å, respectively, and R_{free} values were better than 0.24 (Table 2). The conditions and analyses were the same as for the unmodified scURO-D protein described above. The scURO-D(GY) structure superimposes on 332 of 357 pairs of C^{α} atoms of scURO-D with an RMSD of 0.280 Å. The scURO-D(FY) and scURO-D(YF) structures superimpose on 332 of 357 pairs of C^{α} atoms of scURO-D with RMSDs of 0.237 and 0.283 Å, respectively. Inspection of electron density maps indicated, as expected, that all three structures are identical, with the exception of the mutated residue, which is best modeled as a half-occupied Gly and a half-occupied Tyr (scURO-D(GY) and as a half-occupied Tyr and a half-occupied Phe [scURO-D (YF) and scURO-D(FY)]. F217Y is the more debilitating mutation, and these variants were used for primary enzymatic analyses (see the text below), although the Y164G mutation robustly validated the crystallographic assignment of two superimposable scURO-D orientations due to the large number of electrons eliminated in changing from tyrosine to glycine (Supplementary Fig. 2). These structures

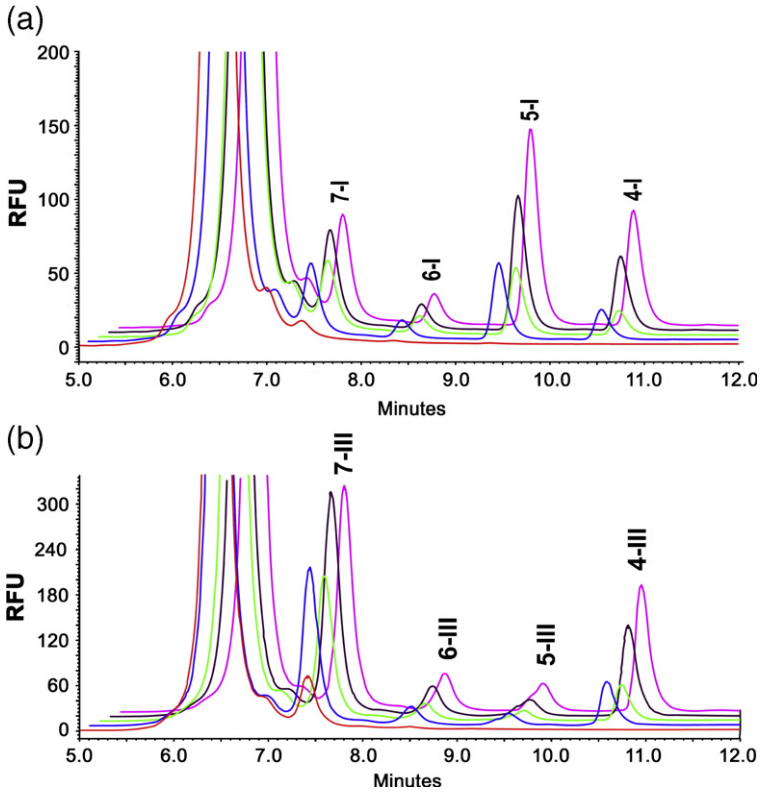

Fig. 4. Product and intermediate profiles of the URO-D reaction. Reaction products of either uro'gen I (a) or uro'gen III (b) from the URO-D enzymatic assay are separated by HPLC; the metabolites heptacarboxyl porphyrin (7), hexacarboxyl porphyrin (6), pentacarboxyl porphyrin (5) and coproporphyrin (4) are labeled with the corresponding isomer designation after the label. Wild-type enzyme (pink), scURO-D (purple), scURO-D(FY) (green), scURO-D(YF) (blue), and scURO-D (FF) (red).

Table 3. Reaction products as percent total decarboxylation

	7-COOH (%)	6-COOH (%)	5-COOH (%)	4-COOH (%)
Isomer I				
URO-D	23	7	42	27
scURO-D	27	8	40	26
scURO-D(FY)	34	10	39	17
scURO-D(YY)	77	15	8	00
scURO-D(YF)	35	10	39	16
Isomer III				
URO-D	53	10	8	29
scURO-D	56	9	8	27
scURO-D(FY)	66	9	7	19
scURO-D(YY)	96	3	1	1
scURO-D(YF)	66	8	7	19

Reaction products expressed as a percentage of the total are represented graphically in Fig. 4a and b as isomer I and isomer III, respectively.

support earlier crystallographic assignments and indicate that the mutations do not have unanticipated structural consequences that might complicate interpretation of biochemical data.

Activities of scURO-D proteins and implications for mechanism

Compared to scURO-D, scURO-D(FY) and scURO-D(YF) display 55% and 62% of full activity, respectively (Table 1). ANOVA indicated that the difference between these values was statistically insignificant. The activity of the scURO-D(YY) mutant was 3% and 15% of scURO-D activity when assayed against uro'gen I and uro'gen III, respectively. The higher activity observed when uro'gen III was used as substrate is likely due to tighter binding of the III isomer substrate.[11,12] The reaction mechanism is unchanged in the mutants, as indicated by a conserved profile of reaction intermediates (Fig. 4, Table 3). If substrate shuttling were required and if one active site were inactive, it is possible that an altered profile of the partially decarboxylated intermediates would accumulate. The peak heights of the species quantified in this HPLC assay change depending on the catalytic activity of the sample tested, but the product-to-intermediate-substrates ratio remains constant in all cases for both uro'gen I and uro'gen III substrates when there is a single active site present. These data indicate that

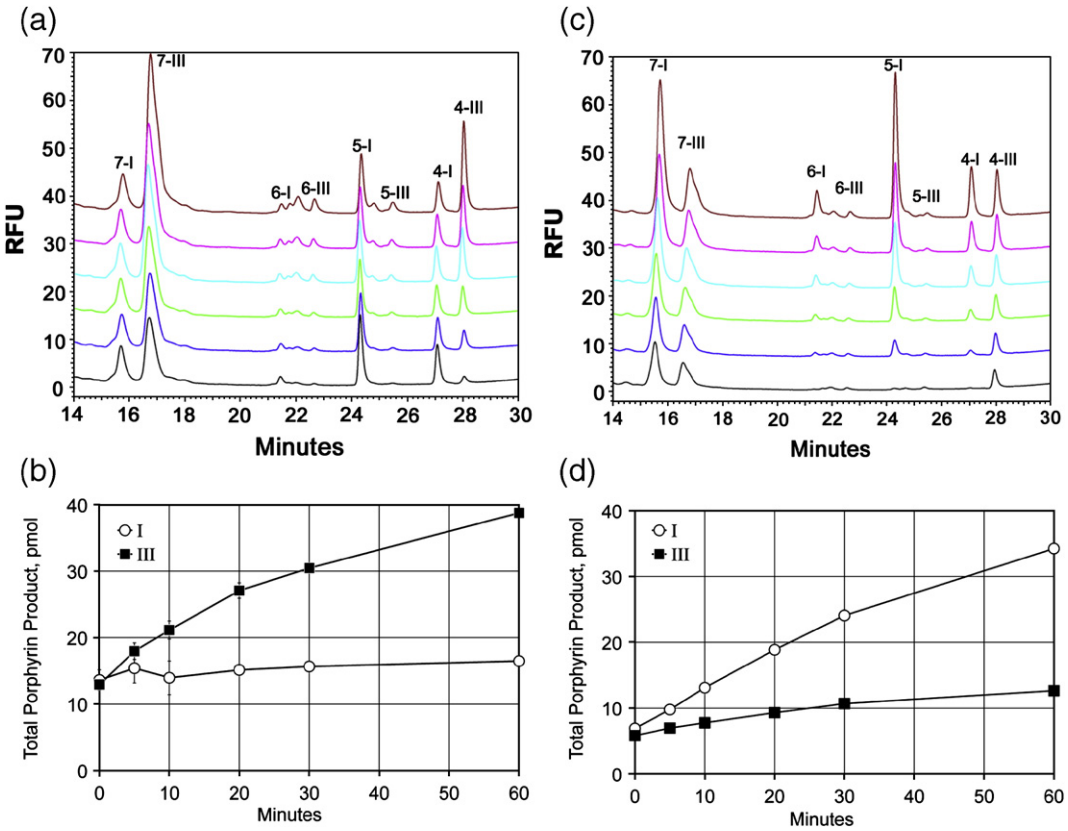

Fig. 5. Product profile of competition assays using wild-type URO-D. (a) The URO-D reaction was started with 5 μM uro'gen I. At 5 min, 45 μM uro'gen III was added. One minute later, the aliquot was removed, and the product profile was measured by HPLC (black trace). The reaction was allowed to continue, and samples were removed for analysis at 5 min (blue trace), 10 min (green trace), 20 min (light blue trace), 30 min (pink trace), and 60 min (brown trace). The metabolites heptacarboxyl porphyrin (7), hexacarboxyl porphyrin (6), pentacarboxyl porphyrin (5) and coproporphyrin (4) are labeled with the corresponding isomer designation (I or III). (b) The total reaction products (in pmol) for isomer I (blue) and isomer III (red) at 1, 5, 10, 20, 30, and 60 min are shown; error bars represent three independent samples. (c and d) Data from an identical experiment where 5 μM uro'gen III was used initially, followed by the addition of 45 μM uro'gen I.

mutation of F217 does not affect substrate binding and release for any of the intermediate products in the URO-D assay when juxtaposed to a wild-type active site, and that the two catalytic centers of the URO-D dimer are functionally independent. This implies that the dimeric structure has been conserved evolutionarily for reasons other than catalytic chemistry, with one possibility being that formation of the dimer interface stabilizes the active-site cleft geometry because residues at the interface also line the active-site cleft.

Wild-type URO-D has a reported K_m of 0.80 μM for uro'gen I and a K_m of 0.35 μM for uro'gen III, suggesting that binding is approximately two times tighter for the III isomer.[11] An enzymatic assay, started using 5 μM uro'gen I as substrate, displayed the formation of all the reaction intermediates (heptacarboxyl-porphyrin, one decarboxylation; hexacarboxyl-porphyrin, two decarboxylations; pentacarboxyl-porphyrin, three decarboxylations) and the product copro'gen (4-COOH) within 5 min (Fig. 5a and b). At 5 min, uro'gen III was added at 45 μM, and continued accumulation of intermediates and products was monitored. Upon uro'gen III addition, the peak areas of the I isomer reaction intermediates/products remained essentially constant, but the peak areas for the III isomer intermediates/products continued to increase with time of incubation. The same is true if decarboxylation of uro'gen III is quenched with uro'gen I after 5 min (Fig. 5c and d). These observations indicate a mechanism in which the intermediates release and rebind to the enzyme on each successive decarboxylation. If the intermediates for the initial isomer that were present at the time of dilution were bound by URO-D and unable to exchange until the completion of all decarboxylation reactions, the amount of coproporphyrin corresponding to the initial isomer would continue to accumulate after dilution with the second substrate. These data support the conclusion that reaction intermediates are released from the enzyme rather than shuttled to the partner active site of the dimer for the next step in the formation of the ultimate product copro'gen.

Because the dimeric structure of URO-D juxtaposes subunit active-site clefts, shuttling between subunit active sites would provide an appealing mechanism to bind the physiologically relevant III isomer substrate and 7-COOH intermediate with equivalent geometry and without an intervening dissociation. Nevertheless, our observations with single-chain variant URO-D proteins demonstrate that substrate shuttling between subunits is not required for catalysis and that intermediates are released, equilibrate with the bulk solvent, and rebind. There are no data to support an obligate substrate shuttling mechanism where the substrate is transferred in a "ping-pong" fashion between active sites, as indicated by competition experiments. The observed strict conservation of URO-D dimerization between species as diverse as the human species and the plant *Nicotiana tabacum*[13] may reflect the location of the dimer interface adjacent to the active site, with residues at the interface also lining the active-site cleft. In this sense, dimerization might be viewed as essential to URO-D activity because it creates a cleft in a $(\beta/\alpha)_8$ protein that is large enough to accommodate a tetrapyrrole substrate.

Materials and Methods

Linking the C-terminus of one URO-D monomer to the N-terminus of a second URO-D monomer

A pET16b vector (Novagen, Madison, WI) containing a single copy of URO-D fused in-frame behind a 21-residue HIS was used as a starting plasmid. An XhoI site was added to the 3′ end of the coding region, removing the stop codon. QuikChange mutagenesis protocol (Stratagene, La Jolla, CA) was used for all plasmid mutageneses. The NdeI-to-XhoI fragment of URO-D was cloned into pTYB1 (New England Biolabs, Beverly, MA) (Supplementary Fig. 3). In a separate reaction, the region 5′ to the 21-amino-acid HIS, between the XbaI site and the NcoI site, was mutated in two additional rounds to produce a coding region in-frame to the histidine tag. This changed the XbaI site into an XhoI site (Supplementary Fig. 3). The URO-D inserts from both plasmids were sequenced to confirm the presence of all changes. The XhoI-to-BlpI fragment of the second plasmid was cloned into the first plasmid to create the initial URO-D fused to the URO-D coding region, scURO-D. Additional rounds of site-directed mutagenesis were performed to add or remove residues using the QuikChange mutagenesis protocol (Stratagene). All DNA modification enzymes were purchased from Invitrogen (Carlsbad, CA). Sequencing was performed at the University of Utah's Core Sequencing Laboratory. Mutations in the active site of URO-D were introduced into the parent plasmid and sequenced for confirmation. The fragments were subcloned into the scURO-D vector for protein expression.

Protein production

URO-D expression plasmids were transformed in BL-21 (DE3) pLysS cells (Novagen). Proteins were expressed using the Overnight Express system (Novagen), as described by the manufacturer. A 6-L culture was grown for each of the URO-D constructs. After overnight growth, samples were centrifuged at 2500*g* for 15 min. The media were then decanted, and cell pellets were frozen at −80 °C until used.

Cells were thawed in 30 mL of lysis buffer [300 mM NaCl, 50 mM sodium phosphate (pH 6.8), and 10% glycerol] and incubated for 30 min, at 4 °C, with 1.2 mL of 10 mg/mL lysozyme prior to sonication for 4×30 s. Samples were returned on ice for 2 min between pulses. The membrane fraction was removed by centrifugation at 12,000*g* for 30 min. The supernatant was loaded onto a 1-mL Ni^{2+}-NTA (Qiagen, Chatsworth, CA) column at 4 °C. The column was washed with 40 mL of buffer A [300 mM NaCl, 50 mM sodium phosphate (pH 6.8), 10% glycerol, and 1 mM β-mercaptoethanol], followed by elution of the protein in 30 mL of buffer A with the addition of 250 mM imidazole. Fractions containing purified recombinant URO-D were dialyzed against 4 L of 20 mM Tris (pH 7.0) and 5% glycerol. The protein concentration was determined using BCA protein

reagents (Pierce, Rockford, IL). For crystallization, proteins were concentrated to 25 mg/mL using Centriprep concentrators (Amicon, Beverly, MA).

Analytical ultracentrifugation

Equilibrium sedimentation data were collected using a Beckman XL-A analytical ultracentrifuge. The sample buffer contained 50 mM Tris (pH 7.5) and 1 mM β-mercaptoethanol. v_{bar} and solvent density were calculated to be 0.7286 and 1.00379, respectively. The samples were scanned at 280 nm every 20 min until no changes were detected and the samples were determined to be at equilibrium. Five independent scans were collected. Data were merged and processed using the Heteroanalysis software.[14]

URO-D assay

The assay for URO-D activity with uro'gen I as substrate was adapted from the method described by Phillips and Kushner.[15] The uro'gen I substrate was enzymatically produced in a mixture containing 360 μM porphobilinogen, 75 mM Tris (pH 7.7), 7.5 mM dithiothreitol, and 3–5 μg/mL purified recombinant porphobilinogen deaminase. This reaction generates 30–35 nmol of uro'gen I in 35 min at 37 °C in the dark. All subsequent steps were carried out either in the dark or under red darkroom light. To prepare uro'gen III, the reaction mixture (described above) also contained 1 μg/mL purified recombinant uro'gen III synthase. Following substrate generation, the pH of the reaction was changed to 6.8, which was optimal for the URO-D reaction, by the addition of 20 μL/mL of 150 mM KH_2PO_4 (pH 5.0).

A sample of 120 μL of substrate was added to 80 μL of enzyme solution that contained 0.4 μg of URO-D and 8 μg of bovine serum albumin in 50 mM potassium phosphate (pH 6.8). The resulting 200-μL assay mixture was incubated at 37 °C for 30 min in the dark, and the reaction was terminated by adding 200 μL of 3 M HCl. Porphyrinogens in the assay mixture were oxidized to porphyrins by exposure to UV light for 30 min or to white light for approximately 2 h. The acidified sample was centrifuged at 14,000*g* for 10 min to remove precipitated proteins, and products were analyzed by HPLC (see the text below).

Isomer competition assay

Uro'gen I and uro'gen III were prepared as described.[16] One microgram of URO-D was incubated with 5 μM uro'gen I for 5 min, whereupon a sample was removed for analysis and 45 μM of uro'gen III was added to the reaction mixture, with additional samples removed for analysis at 1, 5, 10, 20, 30, and 60 min. Reaction products were separated by HPLC, and peaks for each of the intermediate substrates were quantified. An identical experiment was run starting with 5 μM uro'gen III, and then 45 μM uro'gen I was added at 5 min, with intermediate time points as described above.

HPLC of porphyrins

A 25-μL sample of the assay products was injected into a reverse-phase HPLC system consisting of a Waters 2795 Separations module, a μBondapak C18 column (3.9 mm×300 mm), and a Waters 474 scanning fluorescence detector set at 404 nm excitation and 618 nm emission to resolve the various porphyrins. The flow rate was set at 1.0 mL/min. Two solvents were used: solvent A consisted of 50 mM sodium phosphate (pH 4.5) in 50% vol/vol methanol and water, while solvent B consisted of 100% methanol. The millivolt signals detected for the various porphyrins were individually compared with those in a standard solution that contained 62.5 pmol each of uroporphyrin, heptacarboxyl-porphyrin, hexacarboxyl-porphyrin, pentacarboxyl-porphyrin, coproporphyrin, and mesoporphyrin per 25-μL injection. Chromatograms were processed using the Waters Empower software.

Crystal growth and data collection

scURO-D crystallized isomorphously to the native protein at room temperature (~21 °C) under the same conditions as previously identified for wild-type URO-D.[6] The reservoir (500 μL) comprised 1.5 M sodium citrate (pH 6.5). The crystallization drop was prepared by mixing 5 μL of the URO-D protein solution (25 mg/mL) with 3 μL of the reservoir solution. Crystals typically grew in 3–10 days.

Prior to data collection, crystals were transferred to 1.7 M sodium citrate (pH 7.0) and 5% glycerol for 2 min, suspended in a nylon loop, and plunged into liquid nitrogen. Crystals were maintained at 100 K during data collection. Data were integrated and scaled using DENZO and SCALEPACK.[17] Data were phased directly using a model of the URO-D apo-enzyme monomer [Protein Data Bank (PDB) entry 1URO]. The model was optimized by rigid-body minimization and positional and *B*-factor refinement using REFMAC.[18,19] Model building was performed using O.[20] Figures were prepared using PyMOL.[21]

Accession numbers

Coordinates and structure factors have been deposited in the PDB with accession numbers 3GVQ (scURO-D), 3GVR [scURO-D(GY)], 3GVV [scURO-D(FY)], and 3GVW [scURO-D(YF)].

Acknowledgements

This work was supported by National Institutes of Health grants RO1 DK20503, P30 DK072437, and GM 56775. We thank Dr. Steve Alam for assistance with preparation of the samples and analysis of the data from analytical ultracentrifugation, and Hector Bergonia for HPLC analysis of porphyrins. University of Utah Core Laboratories, supported in part by CA 42014, were used for DNA sequencing and oligonucleotide production. The authors are grateful for assistance with data collection and crystal analysis provided by the use of synchrotron facilities at The National Synchrotron Light Source (Brookhaven National Laboratories, supported by the US Department of Energy, Office of Science, Office of Basic Energy Sciences, under contract no. DE-AC02-98CH10886) and The Stanford Synchrotron Radiation Lightsource (operated by Stanford University on behalf of the US Department of Energy, Office of Basic Energy Sciences).

Supplementary Data

Supplementary data associated with this article can be found, in the online version, at doi:10.1016/j.jmb.2009.04.013

References

1. Jackson, A. H., Sancovich, H. A., Ferrmolas, A. M., Evans, N., Games, D. E., Matlin, S. A. *et al.* (1976). Macrocyclic intermediates in the biosynthesis of porphyrins. *Philos. Trans. R. Soc. London*, **273**, 191–206.
2. McLellan, T., Pryor, M. A., Kushner, J. P., Eddy, R. L. & Shows, T. B. (1985). Assignment of uroporphyrinogen decarboxylase (UROD) to the pter→p21 region of human chromosome 1. *Cytogenet. Cell Genet.* **39**, 224–227.
3. Phillips, J. D., Jackson, L. K., Bunting, M., Franklin, M. R., Thomas, K. R., Levy, J. E. *et al.* (2001). A mouse model of familial porphyria cutanea tarda. *Proc. Natl Acad. Sci. USA*, **98**, 259–264.
4. Anderson, K. E., Sassa, S., Bishop, D. F. & Desnick, R. J. (2001). Disorders of heme biosynthesis: x-linked sideroblastic anemia and the porphyrias. In *The Metabolic and Molecular Bases of Inherited Disease* (Scriver, C. R., Beaudet, A. L., Sly, W. S. & Valle, D., eds), pp. 2991–3062, 8th edit. McGraw-Hill, New York.
5. Phillips, J. D., Whitby, F. G., Kushner, J. P. & Hill, C. P. (1997). Characterization and crystallization of human uroporphyrinogen decarboxylase. *Protein Sci.* **6**, 1343–1346.
6. Whitby, F. G., Phillips, J. D., Kushner, J. P. & Hill, C. P. (1998). Crystal structure of human uroporphyrinogen decarboxylase. *EMBO J.* **17**, 2463–2471.
7. Phillips, J. D., Whitby, F. G., Kushner, J. P. & Hill, C. P. (2003). Structural basis for tetrapyrrole coordination by uroporphyrinogen decarboxylase. *EMBO J.* **22**, 6225–6233.
8. Silva, P. J. & Ramos, M. J. (2005). Density-functional study of mechanisms for the cofactor-free decarboxylation performed by uroporphyrinogen III decarboxylase. *J. Phys. Chem. B*, **109**, 18195–18200.
9. Nicholls, C. D., McLure, K. G., Shields, M. A. & Lee, P. W. (2002). Biogenesis of p53 involves co-translational dimerization of monomers and post-translational dimerization of dimers. Implications on the dominant negative effect. *J. Biol. Chem.* **277**, 12937–12945.
10. Phillips, J. D., Parker, T. L., Schubert, H. L., Whitby, F. G., Hill, C. P. & Kushner, J. P. (2001). Functional consequences of naturally occurring mutations in human uroporphyrinogen decarboxylase. *Blood*, **98**, 3179–3185.
11. de Verneuil, H., Grandchamp, B. & Nordmann, Y. (1980). Some kinetic properties of human red cell uroporphyrinogen decarboxylase. *Biochim. Biophys. Acta*, **611**, 174–186.
12. de Verneuil, H., Sassa, S. & Kappas, A. (1983). Purification and properties of uroporphyrinogen decarboxylase from human erythrocytes. A single enzyme catalyzing the four sequential decarboxylations of uroporphyrinogens I and III. *J. Biol. Chem.* **258**, 2454–2460.
13. Martins, B. M., Grimm, B., Mock, H. P., Huber, R. & Messerschmidt, A. (2001). Crystal structure and substrate binding modeling of the uroporphyrinogen-III decarboxylase from *Nicotiana tabacum*. Implications for the catalytic mechanism. *J. Biol. Chem.* **276**, 44108–44116.
14. Cole, J. L. (2004). Analysis of heterogeneous interactions. *Methods Enzymol.* **384**, 212–232.
15. Phillips, J. D. & Kushner, J. P. (1999). Measurement of uroporphyrinogen decarboxylase activity. In *Current Protocols in Toxicology* (Maines, M. D., Costa, L. G., Reed, D. J., Sassa, S. & Sipes, I. G., eds), pp. 8.4.1–8.4.13, John Wiley & Sons, Inc., New York.
16. Bergonia, H. A., Phillips, J. D. & Kushner, J. P. (2009). Reduction of porphyrins to porphyrinogens with palladium on carbon. *Anal. Biochem.* **384**, 74–78.
17. Otwinowski, Z. & Minor, W. (1997). Processing X-ray diffraction data in oscillation mode. In *Methods in Enzymology* (Carter, C. & Sweet, R., eds), vol. 276, pp. 307–326. Academic Press, New York.
18. Murshudov, G. N. (1997). Refinement of macromolecular structures by the maximum-likelihood method. *Acta Crystallogr. Sect. D*, **53**, 240–255.
19. Murshudov, G. N., Vagin, A. A. & Dodson, E. J. (1997). Refinement of macromolecular structures by the maximum-likelihood method. *Acta Crystallogr. Sect. D*, **53**, 240–255.
20. Jones, T. A., Zou, J. Y., Cowan, S. W. & Kjeldgaard, M. (1991). Improved methods for building protein models in electron density maps and the location of errors in these models. *Acta Crystallogr. Sect. A*, **47** (Pt 2), 110–119.
21. DeLano, W. L. (2002). The PyMOL Molecular Graphics System DeLano Scientific, San Carlos, CA, USA; http://www.pymol.org, ed.